Universiteit
Leiden
The Netherlands

Towards in-cell structural study of light-harvesting complexes : an investigation with MAS-NMR

Azadi Chegeni, F.

Citation
Azadi Chegeni, F. (2019, March 12). *Towards in-cell structural study of light-harvesting complexes : an investigation with MAS-NMR*. Retrieved from https://hdl.handle.net/1887/69726

Version:	Not Applicable (or Unknown)
License:	Licence agreement concerning inclusion of doctoral thesis in the Institutional Repository of the University of Leiden
Downloaded from:	https://hdl.handle.net/1887/69726

Note: To cite this publication please use the final published version (if applicable).

Cover Page

Universiteit Leiden

The handle http://hdl.handle.net/1887/69726 holds various files of this Leiden University dissertation.

Author: Azadi Chegeni, F.
Title: Towards in-cell structural study of light-harvesting complexes : an investigation with MAS-NMR
Issue Date: 2019-03-12

CHAPTER 3

Conformational dynamics of photosynthetic light- harvesting complex II in native thylakoid membrane

This work is available as preprint: Azadi Chegeni F., Ward. E. M., Perin G., Simionato D., Morosinotto T., Baldus, M., Pandit A. bioRxiv.
Doi: https://doi.org/10.1101/288860

Abstract

Photosynthetic light-harvesting antenna complexes (LHCs) of plants, moss and green algae form dynamic switches between light harvesting and excitation-quenched, dissipative states. This mechanism protects the photosynthetic apparatus under light stress via a photo protective membrane response. Herein, we demonstrate the application of solid-state NMR spectroscopy to wild type, heterogeneous thylakoid membranes of *Chlamydomonas reinhardtii* (*Cr.)* and purified *Cr*. Light harvesting Complex II (LHCII) reconstituted in thylakoid lipid membranes, to investigate the structure and dynamics of LHCII in native conditions. We find that membrane-reconstituted LHCII contains sites that undergo fast, large-amplitude motions, including the phytol tails of two chlorophylls. In intact thylakoids, the dynamics of these protein and pigment sites is significantly reduced. Furthermore, plasticity is observed in the N-terminal stretch and in the trans-membrane helical edges facing the thylakoid lumen. We conclude that LHCIIs contain flexible sites but that their conformational dynamics is constrained *in vivo*, implying that changes in the physicochemical environment are required to enable switching between different conformational states. *In situ* NMR spectroscopy opens a new route to investigate the plasticity of light-harvesting complexes and their seminal role in biological regulation mechanisms such as membrane state transitions, non-photochemical quenching or post-translational modifications.

Introduction

Multi-pigment protein complexes in plants, moss, and photosynthetic algae perform delicate photo-physical and chemical tasks. These processes are highly regulated by the conformational flexibility of the proteins and their interplay within a dynamic thylakoid membrane environment [1-2]. Obtaining atomic-level structures of these complexes under physiological conditions is an essential step towards understanding the molecular mechanisms that regulate the excitation energy flow. To understand the molecular mechanisms that regulate photosynthesis, the most abundant, peripheral antenna complex, Light Harvesting Complex II (LHCII), has been studied extensively and the conformational switch of LHCII has been the topic of much debate [2-12]. Single-molecule fluorescence studies have demonstrated that individual LHCII complexes can fluctuate between light harvesting and dissipative states [4, 7] and MD (Molecular Dynamics) simulations on LHCII in a lipid bilayer [9] suggest that the N-terminal region is highly disordered and could modulate excitation quenching. Results from single-molecule data have been combined with

structure-based data on photosystem II supercomplexes to propose fluctuating antenna models for excitation energy transfer, in which individual LHCs continuously alternate between fluorescent and quenched states. Furthermore, protein solvation, vibration-induced coherences and structural disorder have been put forward as functional design principles by which antenna pigment-protein assemblies can direct and optimize the excitation energy transfer flow. The conformational states and dynamics of LHCII however have only been investigated in crystals or detergent solutions [4, 10, 13-14]. These conditions are very different from more native conditions where complexes are stabilized in a lipid bilayer and can interact with other proteins, which has been shown to affect their fluorescent states [15-16]. Moreover, in native thylakoid membranes the antenna proteins are held in specific arrangements within LHCII-Photosystem II super complexes [17]. The presence of zeaxanthin, phase transitions, specific lipids and membrane stacking further controls the conformational dynamics of the individual LHCs [18].

To understand the molecular switch functions of LHCs, and the role of the thylakoid environment in controlling their light-harvesting function, it is essential to study their dynamic behavior in their native setting. Until now, no structure-based methods have been presented that could detect the molecular structure and dynamics of LHCs inside a membrane environment. Herein, we applied solid-state NMR (Nuclear Magnetic Resonance) spectroscopy to study the conformational dynamics of LHCII in lipid bilayers and in native thylakoid membranes. Solid-state NMR spectroscopy has shown to be a powerful tool for atomistic detection of membrane proteins in native membrane or cellular environments. Several *in-situ* and *in-cell* solid-state NMR studies have investigated membrane proteins that were overexpressed in prokaryotic and eukaryotic host-expression systems [19-25]. We take advantage of the fact that our target protein is present at a high natural abundance in thylakoid membranes under native conditions, and demonstrate that LHCII NMR signals can be detected in thylakoids isolated from wild-type eukaryotic *Chlamydomonas reinhardtii* (*Cr.*) green algae cells. Isolated U-^{13}C, ^{15}N *Cr.* LHCII were analyzed that were reconstituted in thylakoid-lipid membranes, to obtain a view on the conformational dynamics of LHCII in a lipid environment. By comparing these data to the spectra of native thylakoid membranes, we uncover marked differences in the conformational dynamics of LHCII, with implications for the role of the thylakoid environment for LHCII function.

Material and Methods

Biosynthetic isotope labeling of *Cr.* cells, thylakoid extraction and LHCII isolation

For the experiments on isolated WT LHCII trimers, *Cr.* cells from strain CW 15 were cultivated and thylakoid membranes were isolated as described in chapter 2. Thylakoid membranes corresponding to 3mg/ml of total chlorophylls, according to the optical density at 680 nm, were unstacked with 50 mM Ethylenediaminetetraacetic acid (EDTA) and solubilized for 20 minutes on ice in 3 ml of final 1.2% *n*-Dodecyl α-D-maltoside (α-DM) in 10 mM Hepes (pH 7.5), after vortexing for 1 minute. The solubilized samples were centrifuged at 15000 × g for 30 minutes to eliminate any unsolubilized material and the supernatant with the photosynthetic complexes was then fractionated by ultracentrifugation in a 0–1 M continues sucrose gradient containing 0.06% α-DM and 10 mM Hepes (pH 7.5), at 141000 x g for 40 hours at 4 ℃. The green fraction corresponding to LHCII proteins was harvested with a syringe and Chl concentration adjusted to 2mg/ml with buffer (50 mM Hepes, 5 mM $MgCl_2$, pH 7.5). LHCII proteins solubilized in α-DM were reconstituted in lipid membranes whose composition mimics the native thylakoid membrane (47% monogalactosyldiacylglycerol (MGDG), 12% sulfoquinovosyldiacylglycerol (SQDG), 14% phosphatidylglycerol (PG) and 27% digalactosyldiacylglycerol (DGDG)) with a protein-to-lipid molar ratio of 1:55, according to the method described by Crisafi and Pandit [15]. The chosen protein to lipid ratio is in the range of native protein packing densities in thylakoid membranes, where 70-80% of the membrane surface area is occupied by proteins [26].

For experiments on whole fresh thylakoids, *Cr.* cells were cultivated in TAP medium using ^{13}C labeled sodium acetate in a home-built photo chamber, under continuous illumination with cool white LEDs (~50 µmol m^{-2} s^{-1}). Cells were harvested in the exponential growth phase, centrifuged, and re-suspended in 0.2 volumes of $MgCl_2$ buffer (1 mM $MgCl_2$, 0.1 M Hepes, pH 7.5/KOH, 10% sucrose), and were ruptured by sonication on a 2500 Watt sonicator set at 10 %. The isolation of fresh thylakoids was performed according to Chua and Bennoun [27] with some modifications. This procedure differed from the steps described above for LHCII isolation, by using sucrose gradient layers for purification of the thylakoids in order to obtain more pure fractions. In the procedure, disrupted cells were overlaid with layers of sucrose (3 ml of 1.8 M, 1 ml of 1.3 M, 1 ml of 0.5 M and 5 ml of 0 M) containing 0.1 M Hepes (pH=7.5) and 0.5 M EDTA. The gradients were ultra-centrifuged for one hour at 4 °C in a SW41 swing-bucket rotor (Beckmann) at 24000 rpm (100000×g). The thylakoid fraction was isolated from the dark-green sucrose band (see figure 1A).

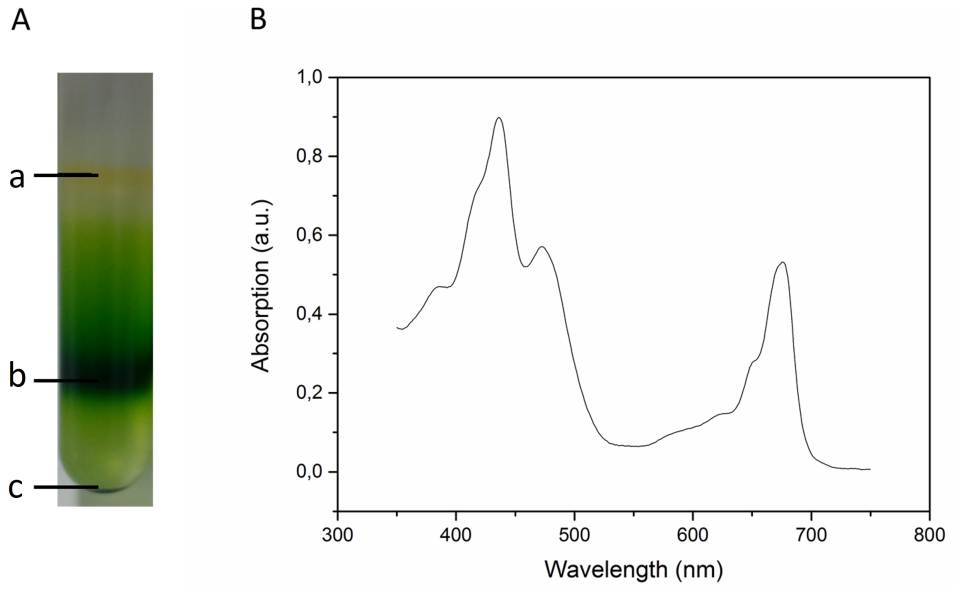

Figure 1. A: Example of thylakoid extraction using a layered sucrose gradient. a. eye spot containing βcarotenes; b. thylakoid membranes; c. cell walls and unbroken cell material. Band b was extracted with a syringe and contained the purified thylakoid fraction. **B:** Absorption spectra of ^{13}C *Cr.* thylakoid membranes. The Q_y absorbance bands of Chl *a* and *b* at are distinguished at 672 and 650 nm respectively, and carotenoids and Chl higher-energy states contribute to the spectrum in the region between 400 and 500 nm.

Gel electrophoresis

Coomassie-stained SDS-page was performed using 15% Tris-glycine gels [28]. Samples were solubilized with a solubilization buffer (4×) containing 30% glycerol, 125 mM Tris pH 6.8, 0.1 M dithiothreitol, 9% SDS.

Pigment analysis

The content of individual carotenoids of *npq2* LHCII was determined using HPLC (Beckman System Gold), as described in [29]. The peaks of each sample were identified through the retention time and absorption spectrum [30].

UV/Visible spectroscopy

Absorption spectra were recorded on a Cary 60 UV–visible spectrophotometer (Agilent Technologies) with the wavelength range from 350 to 750 nm.

Preparation of thylakoid-lipid liposomes

LHCII proteins solubilized in α-DM were reconstituted in lipid membranes of which the composition mimics the native thylakoid membrane. 47% MGDG, 12% SQDG, 14% PG and 27% DGDG with a protein-to-lipid ratio of 1:55 [15]. The chosen protein to lipid ratio is in the range of native protein packing densities in thylakoid membranes, where 70-80% of the membrane surface area is occupied by proteins [26]. Thylakoid lipids were dissolved in chloroform and dried into a thin film using a rotary evaporator at 40 ^{o}C. The thylakoid lipids film was hydrated by reconstitution buffer (50mM HEPES, 5mM $MgCl_2$, pH=7.5 and 0.03% β–DM) and were exposed to 10 freeze-thaw cycles. After that, LHCII was inserted into liposomes and detergent was removed by 3 days incubation with bio beads (SM-2, Bio Rad).

Time-resolved fluorescence spectroscopy (TRF) and 77K fluorescence

TRF measurements on LHCII in detergent and in liposomes were performed using a FluoTime 200 (PicoQuant) time-correlated photon counter spectrometer. Samples were hold in a 1×1 cm quartz cuvette that was thermostated at 20 ^{o}C and excited at 440 nm using a diode laser (PicoQuant). Fluorescence decay traces were fitted with multi-exponentials using a χ^2 least-square fitting procedure. 77k fluorescence measurements were performed using a Fluoromax 3, Horiba, Jobin-Yvon. The samples were diluted in 50 mM HEPES, 5mM $MgCl_2$ buffer and cooled in a nitrogen-bath cryostat to 77K. The samples were excited at 440 nm and a bandwidth of 2 nm was used for excitation and emission.

NMR sample preparation

For the LHCII sample, 18 ml of LHCII in liposomes, containing approximately 10 mg LHCII and 1.5 mg Chl (as determined by OD_{680} of the Chls), was pelleted by ultra-centrifugation (223000×g, 4 ^{o}C, 90 min) and transferred to a 3.2 mm solid-state NMR MAS (Magic Angle Spinning) rotor through centrifugation. For the thylakoid sample, 12 ml of fresh thylakoid membrane containing 2 mg Chl and approximately 10 times more in protein content was pelleted by ultra-centrifugation (100000×g, 4 ^{o}C, 45 min) and transferred to a thin-wall 3.2 mm MAS rotor.

Solid-state NMR experiments

Solid-state NMR spectra of U-^{13}C-^{15}N LHCII in proteoliposomes and of ^{13}C-enriched thylakoid membranes were recorded with an ultra-high field 950-MHz ^{1}H Larmor frequency spectrometer (Bruker, Biospin, Billerica) equipped with a triple-channel

^{1}H, ^{13}C, ^{15}N 3.2 mm MAS probe. Typical π/2 pulses were 3 µs for ^{1}H, 5 µs for ^{13}C, and 8 µs for ^{15}N. The ^{1}H/^{15}N and ^{1}H/^{13}C cross-polarization (CP) [31] contact times were 800 µs and 1 ms, respectively, with a constant radio frequency (rf) field of 35 and 50 kHz on nitrogen and carbon, respectively, while the proton lock field was ramped linearly around the n=1 Hartmann/Hahn condition [32]. The ^{15}N/^{13}Ca SPECIFIC-CP transfer[33] was implemented with an optimized contact time of 4.2 ms with a constant lock field of 2.5×ν_r applied on ^{15}N, while the ^{13}C field was ramped linearly (10% ramp) around 1.5×ν_r. ^{1}H decoupling during direct and indirect acquisition was performed using SPINAL64 [34] with ~83 kHz irradiation. The presented 2D ^{13}C-^{13}C PARIS [35] spectra were collected with a mixing time of 30 ms at 17 kHz MAS at a set temperature of -18 °C. The 2D NCA and NCACX experiments [36] were performed on the LHCII sample at 14 kHz MAS frequency and a readout temperature of -18 °C. For the NCACX experiment a PARIS mixing time of 50 ms was used. The *J*-coupling based 2D ^{13}C-^{13}C INEPT-TOBSY [37-38] experiments were recorded at -3 °C with TOBSY mixing of 6 ms at 14 kHz MAS. Spectra were processed with Bruker TopSpin 3.2 (Bruker, Germany) with LPfr linear prediction and fqc mode for Fourier transformation. Spectra were analyzed by Sparky version 3.114 [39] and MestReNova 11.0 (Mestrelab Research SL, Santiago de Compostela, Spain).

NMR chemical shift prediction using a plant-LHCII homology model

Homology models of *Cr.* LHCII were built using the SWISS model web server [40] based on the LHCII crystal structure of spinach and using the Lhcmb1 or Lhcbm2 sequence of *Cr.* LHCII [41]. The Lhcbm sequences and respective PDB models were used as input for SHIFTX2 [42] in order to predict the ^{13}C and ^{15}N chemical shifts. ^{13}C-^{13}C predicted correlation spectra for use in Sparky [39] were generated by FANDAS [43].

Results and Discussion

Biochemical analysis of Cr. thylakoid membranes and of isolated Cr. LHCII trimers

To investigate the occurrence of LHCII in the thylakoid sample, we used the procedure described for the isolation of the LHCII trimers (*i.e.* re-suspending the thylakoids in Hepes buffer with EDTA and α-DM, see material and methods) and ran a sucrose gradient. Figure 2A shows that the most dense sucrose band contains LHCII trimers, indicating that these are the most abundant pigment-containing complexes in the thylakoids. In addition, SDS-page analysis of the purified *Cr.*

thylakoids was compared to the SDS-page analysis of the isolated *Cr.* LHCII sample (figure 2B). Different molecular-weight bands are distinguished for LHCII in the SDS page analysis due to the fact that the LHCII trimers are isomers consisting of different polypeptides with different molecular weights.

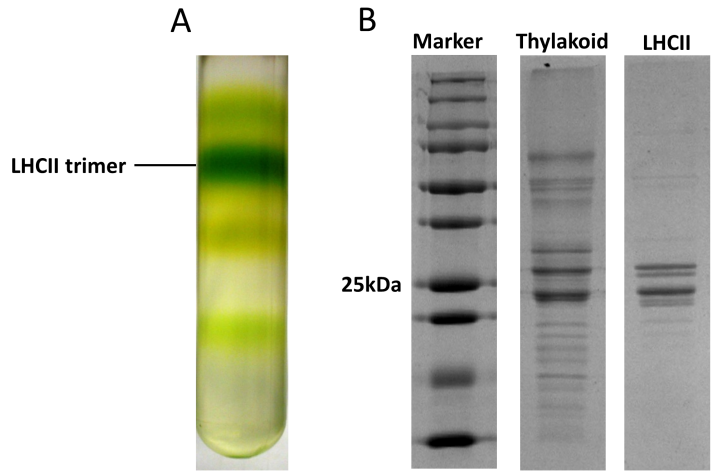

Figure 2. A: Sucrose gradient of *Cr.* thylakoids after solubilizing with 0.6% α-DM, showing the fraction of trimeric LHCII. **B:** SDS page gel analysis of the *Cr.* thylakoid preparation and of isolated LHCII.

The most abundant polypeptides are Lhcbm1, Lhcbm2/7 (Lhcbm2 and Lhcbm7 have identical mature peptide sequences) and Lhcbm3 [44]. In the SDS page gel of the thylakoid sample, two strong bands are observed for LHCII. Based on the relative molecular weights of the polypeptides and other reported analyses, we conclude that the upper band contains Lhcbm3 and the thicker lower band contains Lhcbm1 and Lhcbm2/7 [44-45]. In the SDS-page gel of LHCII two additional smaller bands are observed, which could originate from other Lhcbm polypeptides. The absorbance spectrum of the thylakoid preparation (figure 1B) confirms the presence of protein-associated carotenoids and Chl *a* and *b* pigments. High Performance Liquid Chromatography (HPLC) was performed to determine the pigment composition of LHCII as described previously [46]. The HPLC data show that *Cr.* LHCII proteins bind Chl *a* and *b*, lutein, neoxanthin or loroxanthin and violaxanthin, together with small traces of betacarotene and antheraxanthin (figure 3).

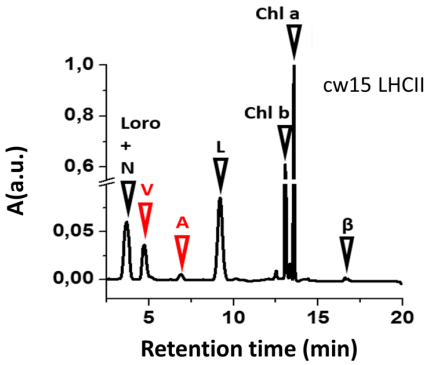

Figure 3. HPLC analysis of trimeric LHCII indicating the presence of violaxanthin.

LHCII were reconstituted into liposomes to mimic the native lipid environment close to those in thylakoid membranes as described in Material and Methods. Under these conditions LHCII form aggregates as reflecting in the 77K fluorscence spectra (figure 4A). Time resolved fluorscence spectra of LHCII before and after insertion into liposomes were measured (figure 4B). Results indicat that the LHCII that are reconstituted in the liposomes are strongly fluorescence quenched. The LHCII in detreget has an average life time of 3.5 ns which reduces to 670 ps after insertion into liposomes.

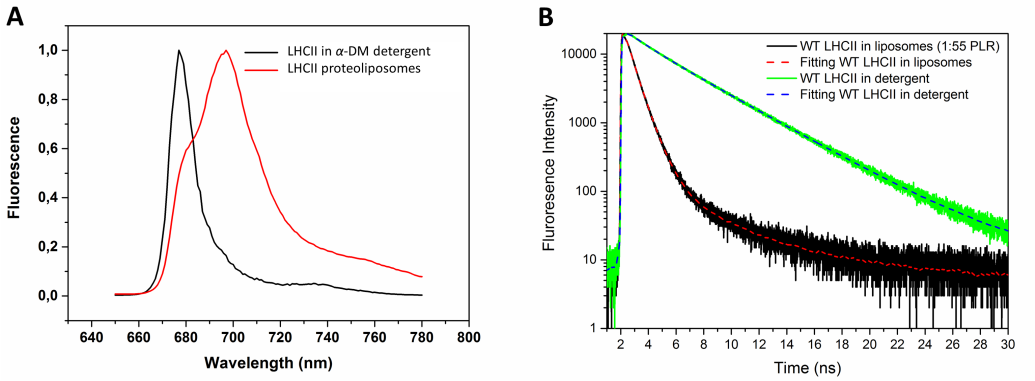

Figure 4. A: 77K fluorescence spectra of LHCII in α-DM detergent (black) and after inserting into liposomes (red). **B:** time resolved fluorescence traces of LHCII in α-DM detergent (green) and of LHCII in liposomes (black).

NMR analysis of LHCII in lipid membranes: detection of resonance from protein, pigment and lipids

Two complementary types of solid-state NMR experiments were employed in this study that are selective for rigid, respectively highly dynamic, molecules. In cross-Polarization (CP) based experiments, ^{1}H-^{13}C or ^{13}C-^{15}N magnetization is transferred via dipolar interaction, which is dependent on the angle between an internuclear vector and the magnetic field. Dipolar-based transfer experiments become inefficient for dynamic molecules, where the dipolar couplings are averaged to zero due to fast tumbling in solution. In INEPT based experiments, magnetization is transferred via *J*-couplings. In the presence of strong motions, where orientation dependent interactions are sufficiently averaged out by magic-angle spinning and fast molecular tumbling, the combination of *J*-based pulse sequences can be employed for screening very flexible parts of large biomolecules [47]. Membrane proteins typically contain large transmembrane stretches with low flexibility, of which the majority of signals are detected in dipolar-based experiments. We first analyzed the membrane-reconstituted LHCII complex in dipolar-based ^{13}C-^{13}C (CC) and ^{15}N-^{13}C (NC) experiments, to verify the incorporation of isotope labels and to identify resonance signals of selective amino-acid and pigment types. Figure 5 presents the CC and NC spectra, showing that several amino-acid types can be identified based on their unique chemical-shift patterns. Helix and coil distributions can be distinguished for alanine, serine, threonine and glycine, as indicated [48], that are in agreement with the known crystallographic structure of plant LHCII which contains both helical stretches and large, coiled loops and tails. In addition to signals originating from the protein content, Chl and carotenoid signals can be identified in regions of the CC spectrum where no protein signals are expected, verifying that these components are also isotopically labeled. Remarkably, in the CC spectrum also a single set of lipid glycerol carbon resonances is observed. It is well-known that each monomer unit of LHCII contains one phosphatidyl-glycerol (PG) lipid, which forms the ligand for Chl611 (nomenclature Liu et al. [13]) and based on their chemical shifts, we attribute the detected lipid resonances in the CC spectrum to the head carbons of LHCII-bound intrinsic PG lipid molecules that were isotope labeled and isolated together with the complex.

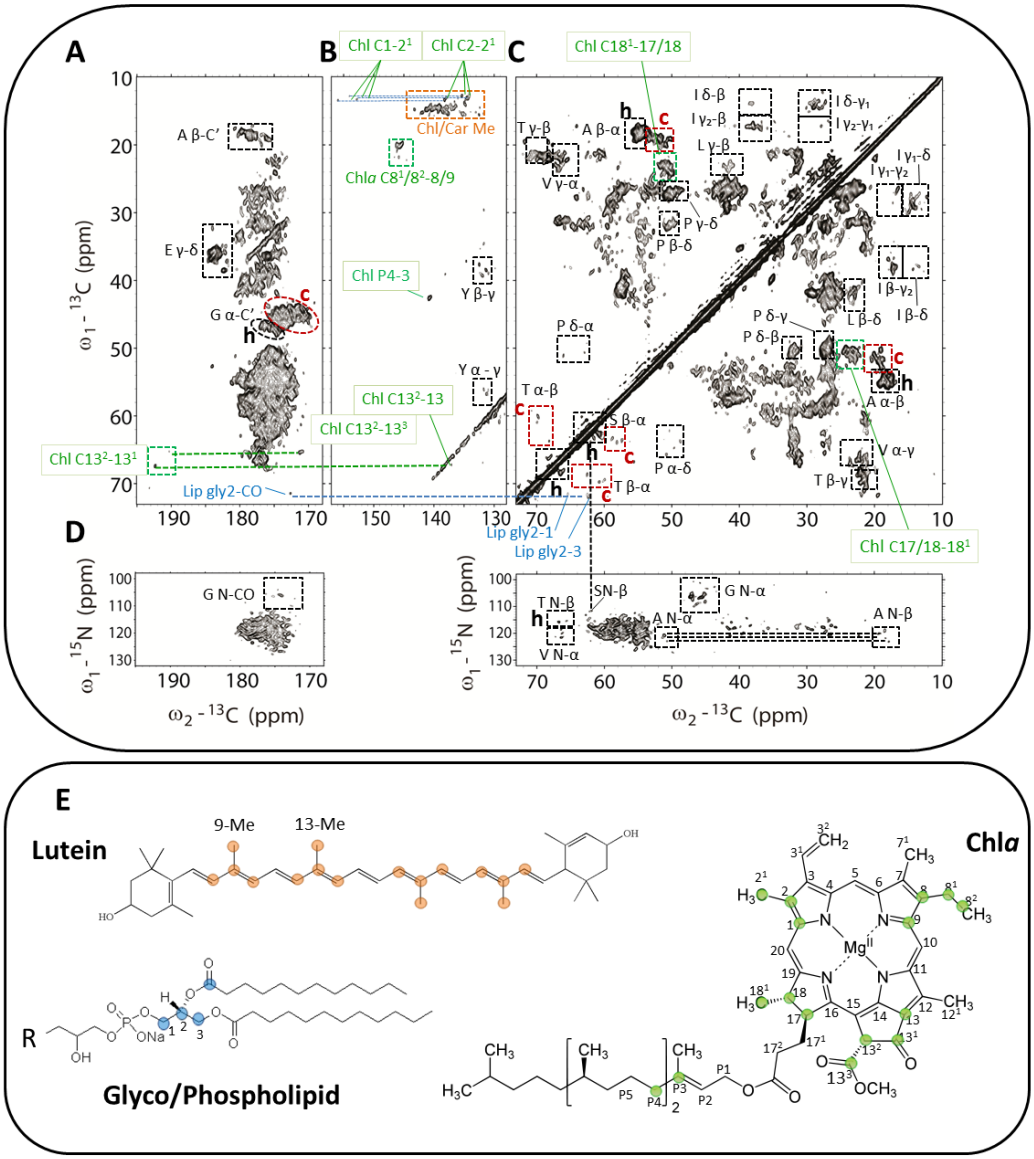

Figure 5. A-C: CP-PARIS ^{13}C-^{13}C spectrum of membrane-reconstituted LHCII. Helix (h) and coil (c) C_α-C_β correlations of Thr, Ser and Ala and C_α -C correlations of Gly are indicated. In addition, protein correlations of Pro, Glu, Ile, and Val are indicated with black contour boxes. Chl, carotenoid and lipid correlations are indicated in respectively green, orange and blue. Their attributed carbon atom types are color-coded in the chemical structures in panel E. **D:** NCACX spectrum of membrane-reconstituted LHCII. N-C_α correlations of Gly, Ser, Ala and Thr are indicated. **E:** Chemical structures of lutein, Chl *a* and of a glyco- or phospholipid molecule with the NMR detected atom types indicated.

Comparison of LHCII structure and dynamics in reconstituted and in native thylakoid membranes: results from dipolar-based experiments

Dipolar-based CC spectra of native thylakoid membranes were collected using parameters that were identical to those used for the isolated LHCII. Figure 6A shows the CC spectrum of LHCII (black) overlaid with the thylakoid spectrum (red). The strong overlap of the two spectra demonstrates, in agreement with the biochemical analysis of our samples, that the most abundant signals in the thylakoid spectra arise from LHCII. Many of the additional peaks that are detected in the thylakoid spectrum can be attributed to lipid signals, confirming that isotope labels are also incorporated into the thylakoid lipids. In particular, multiple resonance signals are detected between 70 and 80 ppm (indicated in figure 5A) that that are outside the region of the protein signals and that are attributed to lipid galactosyl heads.

To have a closer view on the LHCII protein secondary structure in reconstituted and in native membranes, we used correlation signals of Ala, Thr and Ser amino-acid types as reporters for the protein fold. These residue types were chosen because of the clear spectral separation of Ala, Thr and Ser C_α–C_β correlation signals. The distribution of those amino acids along the LHCII polypeptide sequences involves both helical and coil regions, and their resonance signals thus are informative of the fold at several protein sites. The insets of panel 6B, C and D show the Ala, Thr and Ser selective regions. The helical and coil signals fall into separate regions as indicated. To compare the experimental shift correlations with the LHCII structure, three steps were undertaken: (i) models were built for Lhcbm1 and Lhcbm2, the two most abundant polypeptides that form the LHCII trimers in *Cr.*, based on the spinach and pea crystal structures; (ii) C_α and C_β chemical shifts predictions were generated from the Lhcbm1 and Lhcbm2 homology models using the program SHIFTX2 [42] and (iii) simulated CC correlations were generated from the predicted chemical shifts using FANDAS [43]. The resulting chemical shift predictions are overlaid in the inset spectra and shown as cyan and black crosses. Figure 7 presents the spectra of LHCII and thylakoids in the full aliphatic region, with the Lhcbm1 and Lhcbm2 chemical-shift predictions overlaid. The sequences of Lhcbm1 and Lhcbm2, presented in the lower panel in figure 4 show that most of the residues are conserved among Lhcbm1 and Lhcbm2. In the Thr and Ser insets, those residues are labeled together.

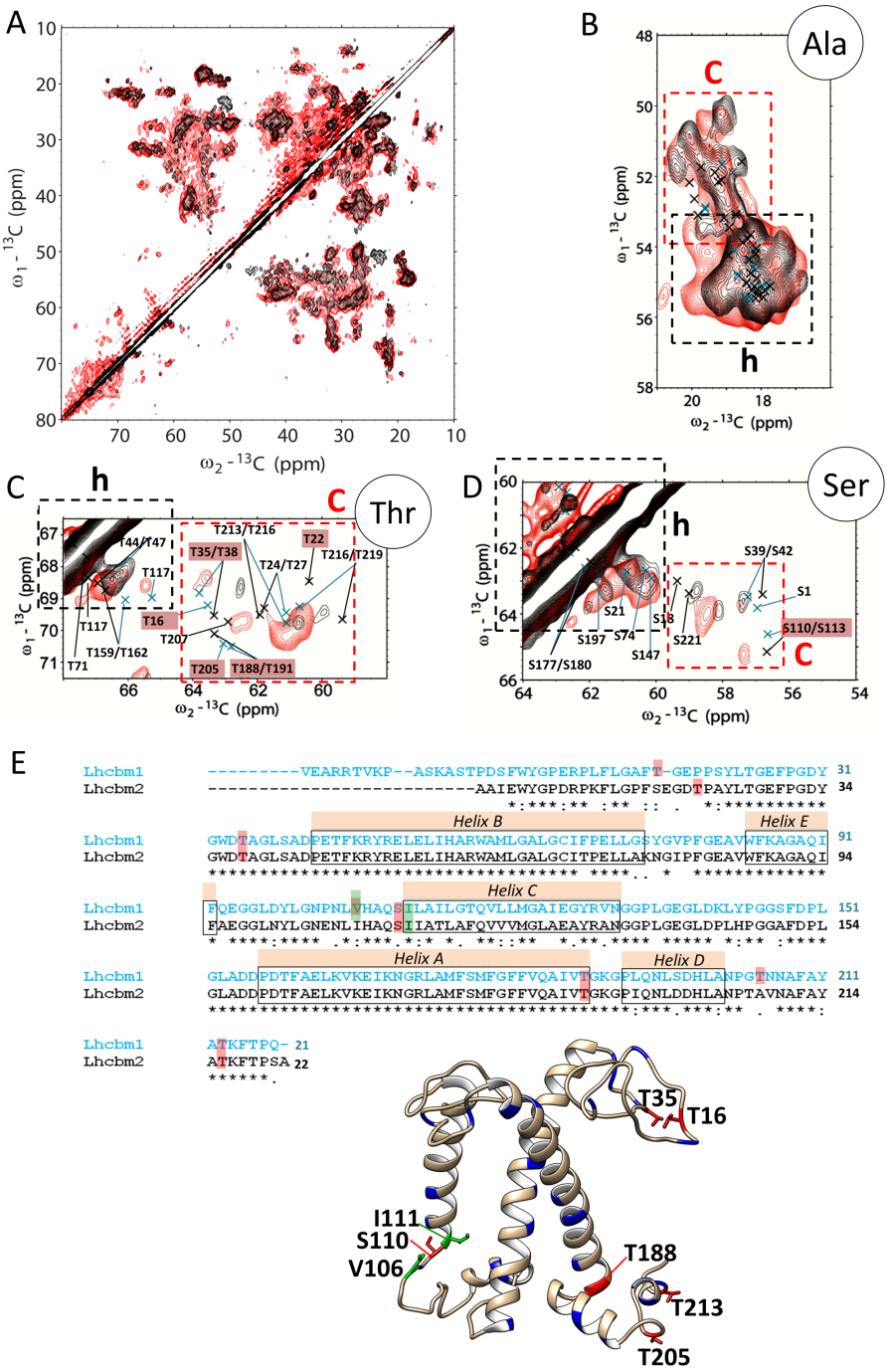

Figure 6. A: CP-PARIS spectrum of thylakoid membranes (red) with the LHCII spectrum (black) overlaid. The insets show the Ala (**B**), Thr (**C**) and Ser (**D**) spectral regions. **E:** chemical-shift predictions of Lhcbm1 (cyan crosses) and Lhcbm2 (orange crosses) are overlaid. Predicted shifts that significantly deviate from experimental correlations in the LHCII spectrum are highlighted in red.

We first focus on the spectrum of isolated LHCII. In panel 6B, C and D the experimental resonances of Ala, Thr and Ser for isolated LHCII are shown in black. If we compare the experimental resonances with the structure-based predictions (cyan and orange), we see that some of the LHCII correlations match closely with predicted correlations, also for non-conserved residues. For instance, experimental peaks are detected close to the predictions for S18 and S221, Ser residues that are found in Lhcbm2 but not in Lhcbm1, which points out that signals of specific polypeptides can be distinguished. However, other predicted signals are not matched by any experimental peak in the LHCII spectrum. For those residues, experimental cross-correlation signals either are not identified because they appear outside their predicted region, or cross resonance signals are not detected because of inefficient cross polarization caused by residue dynamics. Both cases are indicators of protein flexibility. We considered deviations between predicted (ω pred) and experimentally observed (ω exp) correlations significant if $\sqrt{[(\omega_1 \text{ exp} - \omega_1 \text{ pred})^2 + (\omega_2 \text{ exp} - \omega_2 \text{ pred})^2]} \geq 1.2$ ppm and used this as error margin for the chemical-shift predictions. Using this error margin, we find that no experimental signals are observed in the LHCII spectrum within the predicted range for residues T16, T35, S110, T205 and T188 in Lhcbm1 and for T22, T38, S113 and T191 in Lhcbm2. In the LHCII NC spectrum, we observe additional anomalies for V106, I111 and T213 for Lhbm1, and for G20, I114, T191 and T216 for Lhcbm2 (Figure 8). According to the LHCII crystal structures, none of these residues is in direct Van der Waals contact with pigment ligands, excluding that protein-pigment interactions are the cause of the chemical-shift anomalies. The lower panel in Figure 6 shows the Lhcbm1 structure in which residues with deviating shifts are highlighted in red and purple, revealing that the N-terminal stretch at the stromal site and in the CE loop, the edge of helix A, and the C terminus facing the lumen contains flexible protein sites.

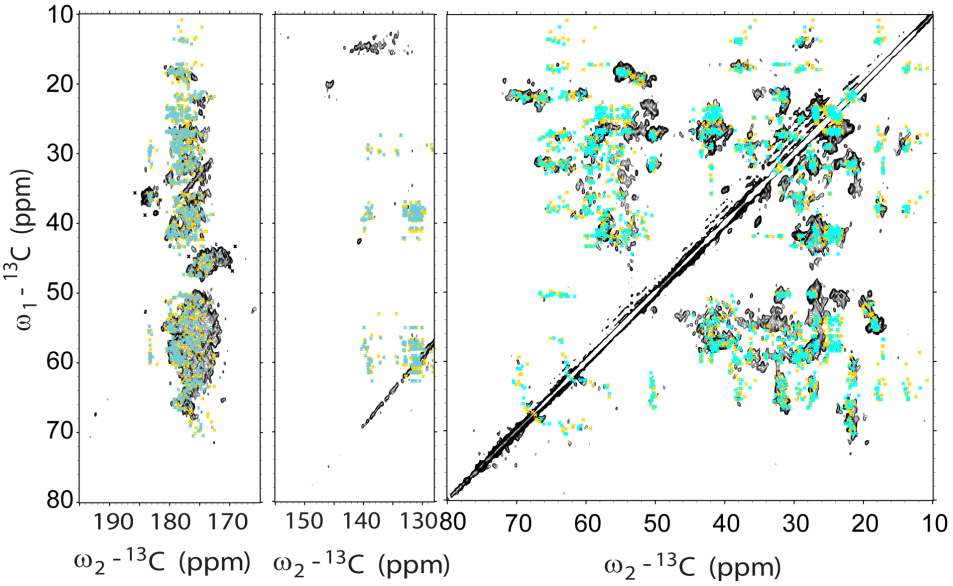

Figure 7. CP-PARIS ^{13}C-^{13}C spectrum of LHCII (black) overlaid with SHIFTX2-generated correlations prediction of Lhcbm1 (cyan) and Lhcbm2 (orange). The spectrum was collected with a mixing time of 30 ms at 17 kHz MAS at a set temperature of -18 ^{o}C.

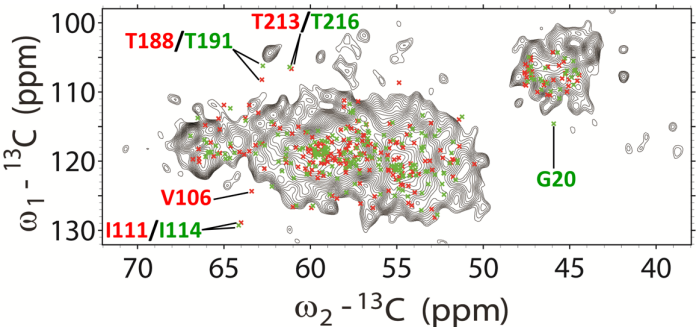

Figure 8. NCA ^{15}N-^{13}C spectrum of LHCII (black) overlaid with predicted correlations of Lhcbm1 (red dots) and Lhcbm2 (green dots). The NCA spectrum was collected at 14 kHz MAS frequency at -18^{o}C, using a mixing time of 800 µs ^{1}H-^{15}N CP step, 4.2 ms for ^{15}N-^{13}C and the number of scans was set to 704. Significant deviations between predicted and experimentally observed cross peaks are observed for Val106, Ile111, Thr188 and Thr213 in Lhcbm1, and in Gly20, Ile114 and Thr216 in Lhcbm2.

Now we compare the above results on LHCII in proteo liposomes with those on LHCII in native thylakoid membranes. In the thylakoid CC spectrum, several signals are shifted compared to the LHCII spectrum. Furthermore, in the Thr and

Ser coil regions stronger signal intensities are observed and additional peaks appear compared to the LHCII spectrum. Comparing the LHCII signals in the thylakoid spectrum (red) to the predicted Thr and Ser chemical-shift predictions, a better overlap is observed. The enhanced signal intensities are indicative of improved cross-polarization efficiencies, signifying that the thylakoid membrane is more rigid than the reconstituted membrane and causes reduced dynamics in LHCII. To test this hypothesis, we proceeded with *J*-based (INEPT-TOBSY) experiments that are selective for molecules with strong dynamics and large-amplitude motions, such as disordered segments.

A comparison of the LHCII and the thylakoid spectrum in other spectral regions is presented in in figure 9 and shows several changes as well. In the CO region, membrane-reconstituted LHCII has an upfield shifted Glu carboxyl peak, indicating a change in the structure or local environment of a Glu residue. In the aromatic region where the chromophore signals are distinguished, chemical shift changes are observed for Chl *a* 8-8^1 resonances, and the LHCII spectrum has three downshifted Me resonance signals (indicated with arrows in the spectrum) that could be attributed to either Chl or carotenoid Me groups, and indicate a change in the local environment of Chl, or possibly of a carotenoid acyl chain.

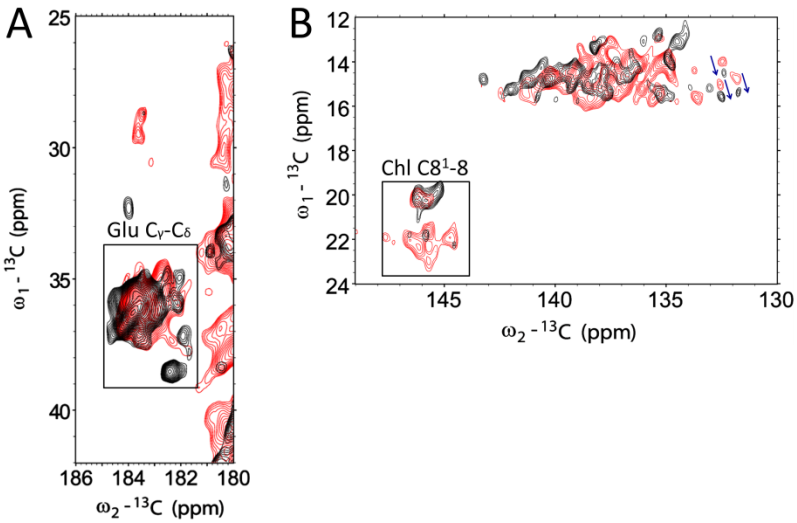

Figure 9. CP-PARIS ^{13}C-^{13}C spectrum of thylakoid membranes (red) with the spectrum of *Cr.* LHCII (black) overlaid. **A:** Carboxyl region showing the Glu C_γ-C_δ correlations. A downfield shift of one Glu in the spectrum of thylakoid membranes is indicated with the arrow. **B:** Carotenoid and Chl region. Downfield shifts of three Me carbons in the spectrum of LHCII are indicated with blue arrows.

J-based experiments reveal reduced LHCII dynamics in native membranes

INEPT based experiments are sensitive for molecules that undergo fast, large-amplitude motions. For biomolecules, these are typically disordered, protein segments with random-coil structures, flexible ligands or mobile lipids with a low degree of segmental order. Figure 10 presents the 2D INEPT-TOBSY spectrum of LHCII (black) overlaid on the INEPT-TOBSY spectrum of thylakoid membranes (red). As expected by the fact that the majority of the protein signals are detected in the dipolar-based spectra, only limited sets of protein signals are detected in the *J*-based spectra that we refer to as "*J*" amino acids. The overlaid spectra clearly show that several *J* amino-acid residues are detected in the INEPT-TOBSY spectrum of LHCII (black), whereas only few residues are detected in the INEPT-TOBSY spectrum of thylakoid membranes (red).

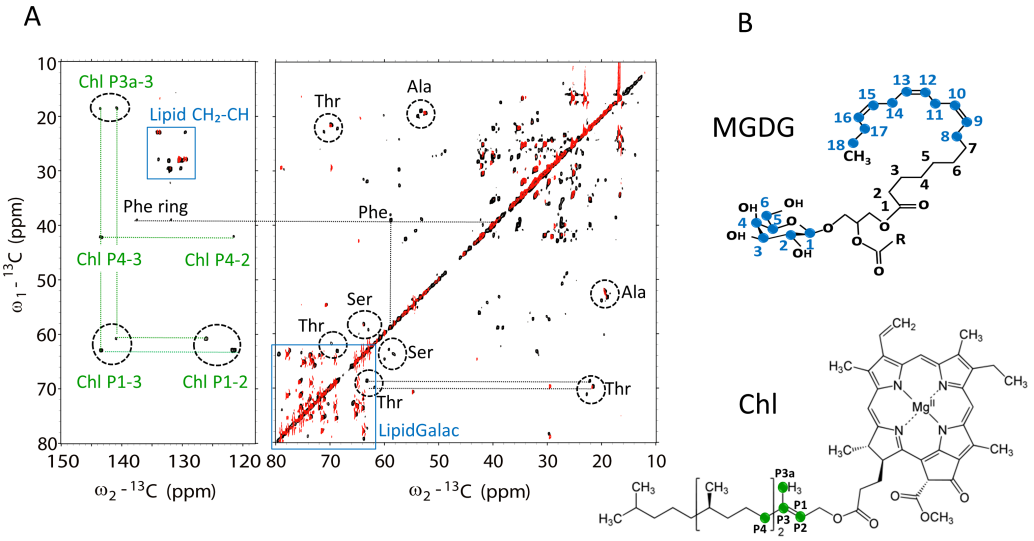

Figure 10. **A:** Overlay of the INEPT-TOBSY spectrum of *Cr.* LHCII (black) and of *Cr.* thylakoids (red). Resonance signals of the two Chls, the lipids and Ala, Thr, Ser, and Phe are indicated. **B:** Chemical structure of MGDG lipid and Chl, highlighting the lipid (blue)and Chl (green) atom types that are detected in the spectra.

We analyzed the chemical-shift correlations in the spectrum of isolated LHCII. We could assign the *J* residues in the LHCII spectrum to Ala, Thr, Ser, Phe, Pro, Val, Lys, Ile, Glu, Asn and Leu amino acid types (3×A,T,S and 1×F,P,V,K,I,E,N,L plus 1 L or D, see table 1 and figure 11). Because these represent residues that display fast and large-amplitude motions, we predict that they are located in the non-

helical loop stretches and in the terminal tails. Interestingly, three distinct peaks are observed for Ala, Thr and Ser, whereas their *J*-based correlations usually tend to strongly overlap. The N terminus of Lhcbm2/7 (AAI, first three amino acids) and the C-terminal stretch of Lhcbm1 starting from A212 (ATKFTPQ) or the equivalent stretch in Lhcbm2/7 and Lhcbm3 (ATKFTPSA) contain many of the observed *J* amino-acid types and we predict that the observed *J* residue signals are from those protein sites. In addition, a Val *J* residue is observed in the LHCII spectrum. The only Val residues outside the helical regions are V106 and V83 that occur in the lumenal loop connecting helix E, and we attribute the Val signal to either one of those two residues. Taking the results together, the *J* analysis of membrane-reconstituted LHCII predicts that fast-amplitude motions could occur for residues in the N- and C-terminus and/or for residues in the lumen loops connecting helix E.

Remarkably, the *J*-based spectrum of LHCII also contains two sets of Chl signals that are assigned to P1, P2, P3, P3a and P4 phytol tail resonances (table 2 and figure 11), indicating the presence of two Chl tails that exhibit strong dynamics. Resonance signals of the Chl phytol chains further towards the tail fall into the aliphatic region (10-30 ppm) and overlap with lipid CH_2 signals. In the LHCII crystal structures, the phytol chain structures of Chl *b* 605 and 606 (nomenclature according to Liu et al. [13]) are not observed, while the other Chl phytol tails are resolved and are involved in stabilizing pigment-protein interactions within the complex. We thus conclude that the observed two sets of Chl phytol resonances in the *J*-based LHCII spectrum belong to the dynamic tails of Chls 605 and 606. Those Chls are close to V106, S110 and I111 that we classified as flexible sites based on analysis of the dipolar-based spectrum in the previous section. Figure 12 shows the LHCII structure with predicted protein and pigment *J* sites indicated in red. Notably, the N-terminal region around T16, (highlighted in the structure) and the C terminus stabilize Chl601 and the xanthophyll-cycle carotenoid Vio (violaxanthin, depicted in the structure) or Zea (zeaxanthin). Flexibility of those sites in isolated LHCII explains that carotenoids in this binding site are loosely bound and easily lost during protein isolation. The region around T35 contains the binding pocket of Lut2 (lutein 2) and flexibility in this site will influence the dynamics of Lut2 and its interaction with Chl601. A comparison of the *J*-based spectrum of LHCII and of the thylakoid membranes shows remarkable differences. The majority of the amino-acid signals in the spectrum of LHCII are not observed in the thylakoid spectrum, and no Chl resonances are observed. In accord with the analysis of the dipolar-based spectra that indicate that LHCII has reduced flexibility in native thylakoid membranes, the *J* analysis reveals that fast-amplitude motions in LHCII are significantly suppressed in the thylakoid membrane environment. We conclude that both small-amplitude motions in LHCII that reduce cross-polarization efficiency, and large-amplitude, segmental motions that enhance INEPT efficiencies, are significantly reduced in the native thylakoid

membranes compared to LHCII in reconstituted membranes. The predicted dynamic sites are close to the binding pockets of Vio or Zea and Lut2 in LHCII, inferring that those LHCII-associated carotenoids have decreased dynamics for LHCII in its native environment compared to LHCII in liposomes.

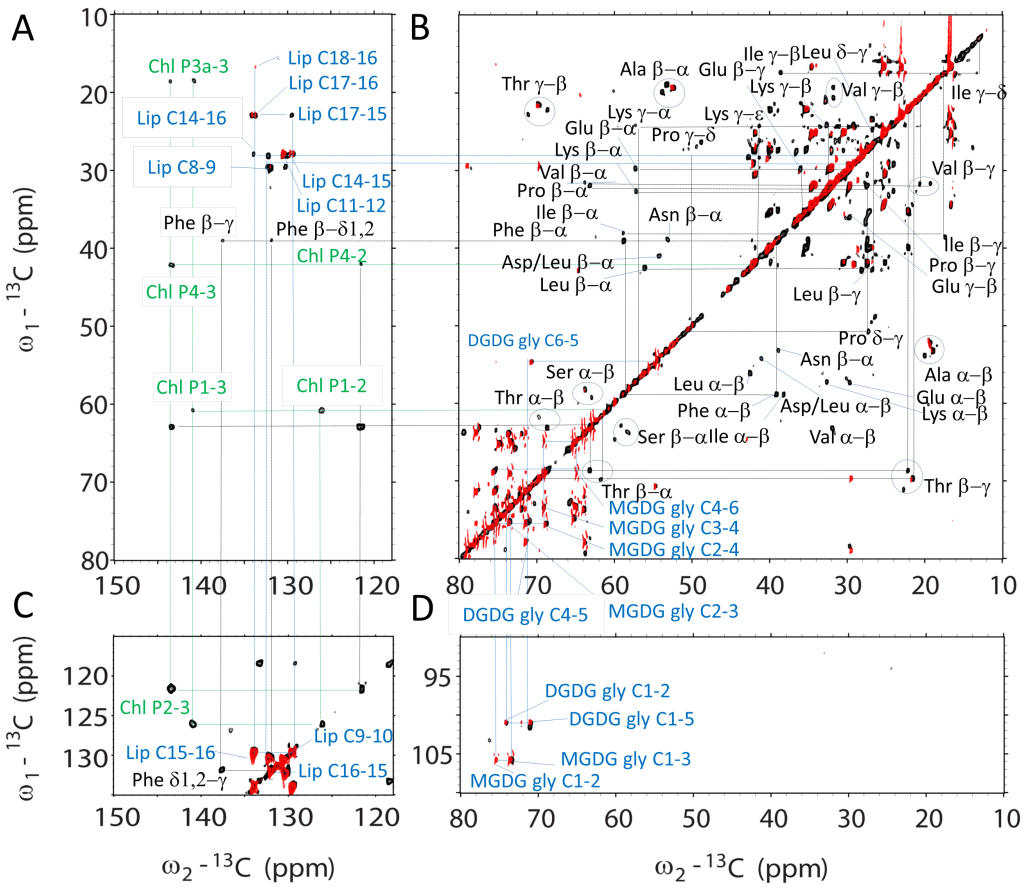

Figure 11. A-D: Overlay of the INEPT-TOBSY spectrum of *Cr.* LHCII (black) and of *Cr.* thylakoids (red). Protein assignments are indicated in black, Chl assignments in green and lipid assignments in blue.

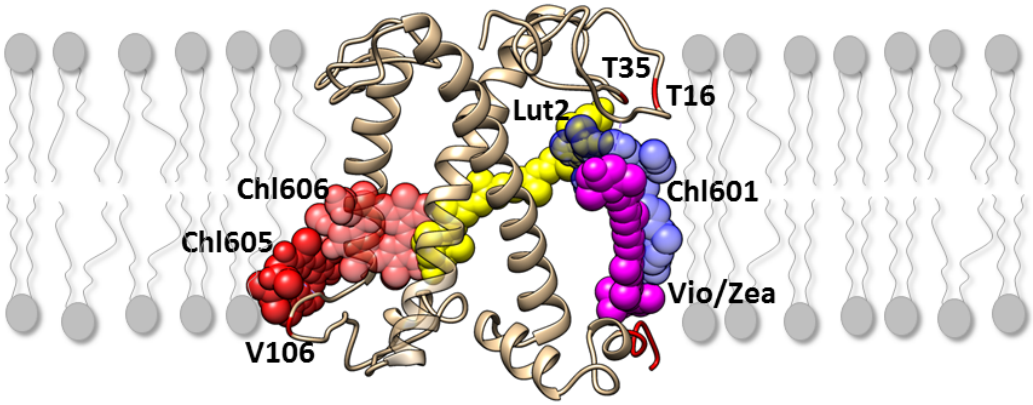

Figure 12. LHCII pigment-protein crystal structure, highlighting flexible protein sites and pigments that are in close vicinity.

Residue type	C_α [ppm]	C_β [ppm]	C_γ [ppm]	C_δ [ppm]	C_ε [ppm]
Ala	52.4	19.3			
	53.3	18.9			
	53.8	19.8			
Thr	61.9	69.7	21.5		
	63.2	68.6	22.2		
		71.1	22.8		
Ser	58.2	63.8			
	59.3	62.9			
	60.0	64.7			
Phe	58.8	39.1	137.5	131.9	
Ile	62.4	38.6	17.4	13.3	
Lys	57.2	32.7	24.2		41.4
Val	63.2	31.9	20.6	19.3	
Glu	57.3	29.7			
Asn	53.1	38.9			
Leu	56.1	42.5			
Pro	63.8	31.5	26.4	48.9	
			27.4	50.8	
			26.9	49.5	
Asp/Leu	54.2	41.0			

Table 1. Assignment of mobile amino-acid residue types detected in the *J*-based INEPT-TOBSY spectrum of membrane-reconstituted U-^{13}C-^{15}N LHCII.

Carbon atom	Chemical shift (ppm) Chl i [ppm]	Chl ii[ppm]
P1	60.8	62.9
P2	121.6	126.1
P3	140.8	143.5
P3a	18.4	18.4
P4	42.5	42.1

Table 2. Assignment of Chlorophyll tail ^{13}C resonance signals detected in the *J*-based INEPT-TOBSY spectrum of membrane-reconstituted U-^{13}C-^{15}N LHCII.

Dynamics of intrinsic lipids

The most abundant lipid types that are found in thylakoid membranes of *Cr.* are the glycolipids MGDG (monogalactosyldiacylglycerol), DGDG (digalactosyldiasylglycerol) and SQDG (sulfoquinovosyl diacylglycerol), and the phospholipid PG (phosphatidylglycerol). An important advantage of our NMR approach, where we investigate native membrane proteins, is that the labels are also incorporated in the membrane lipids, allowing us to identify the nature of lipid molecules that are co-purified with LHCII and to assess their dynamics. Note that the reconstituted lipids in the LHCII proteoliposomes are not isotope labeled and the probability of detecting ^{13}C-^{13}C cross correlations of natural-abundance carbons is very low. The lipid ^{13}C signals that are detected in CC spectra of membrane-reconstituted LHCII therefore must originate from intrinsic lipids that remained associated with the protein complex during the isolation procedure. For LHCII, a specific set of lipid signals attributed to PG was detected in the dipolar-based CC spectrum (Figure 3), indicating that a PG lipid molecule is strongly bound to the complex. LHCII complexes bind one PG lipid per monomer that is essential for ligating Chl611. Together with Chl612 and Chl610, these Chls form the terminal emitter domain of LHCII where excitations accumulate via downhill intra-protein energy-transfer. In the dissipative state, this site has been proposed to form a quenching domain [18]. A recent MD study on LHCII monomers suggested that the dynamic fluctuations of this lipid, which is stabilized by the N-terminal stretch, could modulate Chl611-Chl612 excitonic interactions with consequences for excitation quenching [9]. The appearance of strong lipid PG signals in the dipolar-based spectrum however are indicative of low dynamics. In contrast, multiple lipid signal resonances are observed in the *J*-based CC spectrum of LHCII that arise from glycolipid molecules (figure 9). Resonances of lipid galactosyl heads are

observed in the region between 50-106 ppm that can be assigned to MGDG and to DGDG or SQDG [49] and that are summarized in table 3. The glycolipids must also have been co-purified with LHCII indicating they are associated with the complex. However, their appearance in the INEPT spectrum reveals that they exhibit strong dynamics. We think that the intrinsic glycolipids may have exchanged with the (unlabeled) reconstituted lipids upon insertion of LHCII into the liposomes and are no longer protein bound. The high mobility of the MGDG head atoms does not support the hypothesis of Seiwert *et al.*, who suggested that specific hydrogen-bonding interactions might occur between LHCII and the MGDG galactosyl heads[50].

Carbon atom	**Chemical shift (ppm)**	
	MGDG	**DGDG**
C1	105.9	101
C2	75.4	74.3
C3	73.4	-
C4	68.9	77.7
C5	-	71.1
C6	65	54.6
C7	-	-
C8	130.2	130.2
C9	132.1	132.1
C10	29.6	29.6
C11	27.9	27.9
C12	130.7	130.7
C13	-	-
C14	27.8	27.8
C15	129.6	129.6
C16	133.8	133.8
C17	23.1	23.1
C18	16.66	16.66

Table 3. Assignment of ^{13}C lipid resonance signals detected in the *J*-based INEPT-TOBSY spectrum of membrane-reconstituted U-^{13}C-^{15}N LHCII and in the spectrum of U-^{13}C thylakoid membranes.

The lipid signatures in the NMR spectra of thylakoid membranes provide us with a molecular picture of lipid dynamics inside the membranes. Resonances of different lipid types are detected in both the thylakoid *J*- and the dipolar-based spectrum, showing that the thylakoid membrane contains mobile lipids with low segmental order and immobilized lipids with low dynamics. The results are in agreement with our recent 1D MAS-NMR studies on whole thylakoids and intact cells [46 51]. Owing to better peak separation in 2D spectra, we now can distinguish different

glycolipids on basis of their galactosyl head correlations, and to assign CH-CH_2 correlations of carbons in the unsaturated lipid tails. Because of the dense protein packing in the thylakoid membranes, we expect that the majority of the lipid molecules is constrained by lipid-protein interactions. However the CH-CH_2 correlation signals from the unsaturated glycolipid tails, resonating between 20-35 ppm in ω_1 and between 130-137 ppm in ω_2, only appear in the INEPT spectrum. Seemingly, the unsaturated lipid chains are all mobile and disordered, despite the crowding and overall rigidity of the thylakoid membranes.

Implications for the LHCII conformational switch in vivo

The NMR analysis clearly demonstrates that in thylakoid membranes *in vivo* at ambient temperature the conformational dynamics of LHCII are much more constrained than in thylakoid-mimicking liposome environments *in vitro* and that both fast, large-amplitude and slower motions are suppressed. The organization of LHCII in Photosystem II-LHCII (PSII-LHCII) supercomplexes, and the occurrence of three-dimensional membrane stacks that are not mimicked by the liposome membranes could cause restrained dynamics in LHCII in a thylakoid environment. *Cr.* thylakoid membranes form stacks of 2-3 membrane layers that are stabilized by transversal salt bridges between the stromal sites of LHCII complexes, and are mediated by divalent cations [52]. Moreover, specific arrangements of super complexes occur in the lateral plane of the membrane. According to the cryo-electron microscopy (cryo-EM) structures of *spinach* PSII-LHCII super complexes, Chl605 and the protein AC and EC loops of LHCII are in close contact with the minor antenna proteins CP29 or CP26 [17, 53] and in the low-resolution structures of *Cr.* PSII-LHCII, *Cr.* LHCII trimers are also arranged next to CP29 and CP26 [44].

Our findings call to question whether or not spontaneous fluctuations of individual LHC proteins between different conformational states, as has been observed by single-molecules spectroscopy (SMS) and has been suggested by MD simulations, do occur *in vivo*. With SMS, dynamic transitions were detected for isolated LHCII and conformational fluctuations under those conditions were strong enough to occasionally cross the energetic barriers between different conformational states. According to our analysis, membrane-reconstituted LHCII contains distinct flexible sites that may undergo thermally-induced conformational transitions. LHCII in native, stacked thylakoid membranes however does not display this flexibility. This strongly suggests that *in vivo* under those conditions the LHCs are locked in their specific state, implying that an actinic response is required to temporarily reduce the energetic barriers by alterations in the physicochemical environment. Notably, the thylakoid sample was isolated from cells grown under moderate light conditions and we assume that the thylakoid-embedded LHCII structures represent the light-

harvesting conformation. Thus far this conformational state could only be assessed *in vitro* using isolated proteins in detergent solutions [3-4, 8] of which the dynamic features are not representative of their native states. In *Cr.* green algae, the LHC protein LHCSR is found to be involved in pH-induced non-photochemical quenching under excess light conditions. It is therefore noted here that under the growth conditions used for our experiments, no LHCSR is present in the cells.

Conclusion

In-cell solid-state NMR is a rapid emerging field of research that is confronted with the major challenge of identifying signals from target proteins against the background of all other cell components. We demonstrate that the NMR signals of the major light-harvesting antenna LHCII can be detected of the protein within heterogeneous membranes that still contain the photosynthetic machinery. Moreover, lipid signals can be identified in parallel and signals are detected from different Lhcbm polypeptide types, which are not distinguished in crystallographic and cryo-EM structures. Selective Lhcbm mutants could be used in the future to further identify chemical shift contributions of the different polypeptide types [45]. Through our approach, we could compare the conformational dynamics in LHCII in native thylakoid membranes to its dynamics in reconstituted membranes. The significant differences that are observed underline the importance of molecular investigation of this pigment-protein complex in its native settings, and question whether spontaneous fluctuations between different fluorescent states occur for this protein *in vivo*. Our NMR approach now opens a route to compare the *in-situ* conformational dynamics of LHCII as function of phosphorylation, membrane state transitions and non-photochemical quenching conditions and determine the influence of thylakoid plasticity on the protein molecular conformational states.

References

1. Kirchhoff, H., Structural changes of the thylakoid membrane network induced by high light stress in plant chloroplasts. *Philosophical Transactions of the Royal Society B: Biological Sciences* **2014,** *369* (1640), 20130225.
2. Horton, P.; Ruban, A., Molecular design of the photosystem II light-harvesting antenna: photosynthesis and photoprotection. *Journal of Experimental Botany* **2005,** *56* (411), 365-373.
3. Ruban, A.; Berera, R.; Ilioaia, C.; van Stokkum, I. H. M.; Kennis, J. T. M.; Horton, P.; van Grondelle, R.; Pascal, A.; van Amerongen, H.; Robert, B., Identification of a mechanism of photoprotective energy dissipation in higher plants. *Nature* **2007,** *450* (7169), 575-578.

4. Kruger, T.; Ilioaia, C.; Johnson, M.; AV Ruban; Papagiannakis, E.; Horton, P.; Grondelle, R. v., Controlled Disorder in Plant Light-Harvesting Complex II Explains Its Photoprotective Role. *Biophysical journal* **2012,** *102* (11), 2669-2676.
5. Holt, N.; Zigmantas, D.; Valkunas, L.; Li, X.; Niyogi, K.; Fleming, G., Carotenoid cation formation and the regulation of photosynthetic light harvesting. *Science (New York, N.Y.)* **2005,** *307* (5708), 433-436.
6. Robert, B.; Horton, P.; Pascal, A.; Ruban, A., Insights into the molecular dynamics of plant light-harvesting proteins in vivo. *Trends in plant science* **2004,** *9* (8), 385-390.
7. Schlau-Cohen, G. S.; Yang, H.-Y.; Krüger, T. P. J.; Xu, P.; Gwizdala, M.; van Grondelle, R.; Croce, R.; Moerner, W. E., Single-Molecule Identification of Quenched and Unquenched States of LHCII. *The Journal of Physical Chemistry Letters* **2015,** *6* (5), 860-867.
8. Pandit, A.; Reus, M.; Morosinotto, T.; Bassi, R.; Holzwarth, A.; Holzwarth, A. R., An NMR comparison of the light-harvesting complex II (LHCII) in active and photoprotective states reveals subtle changes in the chlorophyll a ground-state electronic structures. *Biochimica et biophysica acta. Bioenergetics* **2013,** *1827* (6), 738-744.
9. Liguori, N.; Periole, X.; Marrink, S. J.; Croce, R., From light-harvesting to photoprotection: structural basis of the dynamic switch of the major antenna complex of plants (LHCII). *Sci Rep* **2015,** *5*, 15661.
10. Standfuss, A. C.; Terwisscha van Scheltinga, M.; Lamborghini, W.; Kühlbrandt, Mechanisms of photoprotection and nonphotochemical quenching in pea light-harvesting complex at 2.5 Å resolution. *EMBO journal* **2005,** *24* (5), 919-928.
11. Papadatos, S.; Charalambous, A. C.; Daskalakis, V., A pathway for protective quenching in antenna proteins of Photosystem II. *Scientific Reports* **2017,** *7* (1), 2523.
12. Miloslavina, Y.; Wehner, A.; Lambrev, P. H.; Wientjes, E.; Reus, M.; Garab, G.; Croce, R.; Holzwarth, A. R., Far-red fluorescence: A direct spectroscopic marker for LHCII oligomer formation in non-photochemical quenching. *FEBS Letters* **2008,** *582* (25-26), 3625-3631.
13. Liu, Z.; Yan, H.; Wang, K.; Kuang, T.; Zhang, J.; Gui, L.; An, X.; Chang, W., Crystal structure of spinach major light-harvesting complex at 2.72 Å resolution. *Nature* **2004,** *428* (6980), 287-292.
14. Fehr, N.; Dietz, C.; Polyhach, Y.; von Hagens, T.; Jeschke, G.; Paulsen, H., Modeling of the N-terminal Section and the Lumenal Loop of Trimeric Light Harvesting Complex II (LHCII) by Using EPR. *J Biol Chem* **2015,** *290* (43), 26007-20.
15. Crisafi, E.; Pandit, A., Disentangling protein and lipid interactions that control a molecular switch in photosynthetic light harvesting. *Biochim Biophys Acta* **2017,** *1859* (1), 40-47.
16. Natali, A.; Gruber, J. M.; Dietzel, L.; Stuart, M. C.; van Grondelle, R.; Croce, R., Light-harvesting Complexes (LHCs) Cluster Spontaneously in Membrane Environment Leading to Shortening of Their Excited State Lifetimes. *J Biol Chem* **2016,** *291* (32), 16730-9.
17. Wei, X.; Su, X.; Cao, P.; Liu, X.; Chang, W.; Li, M.; Zhang, X.; Liu, Z., Structure of spinach photosystem II–LHCII supercomplex at 3.2 Å resolution. *Nature* **2016,** *534*, 69.
18. Ruban, A.; Ruban, M.; Duffy, The photoprotective molecular switch in the photosystem II antenna. *Biochimica et biophysica acta. Bioenergetics* **2012,** *1817* (1), 167-181.
19. Ward, M. E.; Wang, S.; Munro, R.; Ritz, E.; Hung, I.; Gor'kov, Peter L.; Jiang, Y.; Liang, H.; Brown, Leonid S.; Ladizhansky, V., In Situ Structural Studies of Anabaena Sensory Rhodopsin in the E. coli Membrane. *Biophysical Journal* **2015,** *108* (7), 1683-1696.
20. Miao, Y.; Qin, H.; Fu, R.; Sharma, M.; Can, T.; Hung, I.; Luca, S.; Gor'kov, P. L.; Brey, W. W.; Cross, T. A., M2 Proton Channel Structural Validation from Full Length Protein Samples in Synthetic Bilayers and E. coli Membranes. *Angewandte Chemie (International ed. in English)* **2012,** *51* (33), 8383-8386.
21. Fu, R.; Wang, X.; Li, C.; Santiago-Miranda, A. N.; Pielak, G. J.; Tian, F., In situ structural characterization of a recombinant protein in native Escherichia coli membranes

with solid-state magic-angle-spinning NMR. *Journal of the American Chemical Society* **2011,** *133* (32), 12370-3.
22. Kaplan, M.; Narasimhan, S.; de Heus, C.; Mance, D.; van Doorn, S.; Houben, K.; Popov-Celeketic, D.; Damman, R.; Katrukha, E. A.; Jain, P.; Geerts, W. J. C.; Heck, A. J. R.; Folkers, G. E.; Kapitein, L. C.; Lemeer, S.; van Bergen En Henegouwen, P. M. P.; Baldus, M., EGFR Dynamics Change during Activation in Native Membranes as Revealed by NMR. *Cell* **2016,** *167* (5), 1241-1251 e11.
23. Renault, M.; Pawsey, S.; Bos, M. P.; Koers, E. J.; Nand, D.; Tommassen-van Boxtel, R.; Rosay, M.; Tommassen, J.; Maas, W. E.; Baldus, M., Solid-state NMR spectroscopy on cellular preparations enhanced by dynamic nuclear polarization. *Angew Chem Int Ed Engl* **2012,** *51* (12), 2998-3001.
24. Baker, L. A.; Sinnige, T.; Schellenberger, P.; de Keyzer, J.; Siebert, C. A.; Driessen, A. J. M.; Baldus, M.; Grunewald, K., Combined (1)H-Detected Solid-State NMR Spectroscopy and Electron Cryotomography to Study Membrane Proteins across Resolutions in Native Environments. *Structure (London, England : 1993)* **2017**.
25. Shi, P.; Li, D.; Chen, H.; Xiong, Y.; Wang, Y.; Tian, C., In situ (19)F NMR studies of an E. coli membrane protein. *Protein Science : A Publication of the Protein Society* **2012,** *21* (4), 596-600.
26. Kirchhoff, H.; Mukherjee, U.; Galla, H. J., Molecular architecture of the thylakoid membrane: lipid diffusion space for plastoquinone. *Biochemistry* **2002,** *41* (15), 4872-82.
27. Chua, N. H.; Bennoun, P., Thylakoid membrane polypeptides of Chlamydomonas reinhardtii: wild-type and mutant strains deficient in photosystem II reaction center. *Proceedings of the National Academy of Sciences of the United States of America* **1975,** *72* (6), 2175-2179.
28. Laemmli, U. K., Cleavage of Structural Proteins during the Assembly of the Head of Bacteriophage T4. *Nature* **1970,** *227*, 680-685.
29. Färber, A.; Jahns, P., The xanthophyll cycle of higher plants: influence of antenna size and membrane organization. *Biochim. Biophys. Acta* **1998,** *1363*, 47-58.
30. Jeffrey, S. W.; Mantoura, R. F. C.; Wright, S. W., Phytoplankton pigments in oceanography: guidelines to modern methods. *Monogr. Oceanogr. Methodol.* **1997**.
31. Pinest, A.; Gibbyt, M.G.; Waugh, J. S., Proton-enhanced NMR of dilute spins in solids. *The journal of Chemical Physics* **1973,** *69* (2), 569-590.
32. Hartmann, S. R.; Hahn, E. L., Nuclear Double Resonance in the Rotating Frame. *Physical Review* **1962,** *128* (5), 2042-2053.
33. Baldus, M.; Petkova, A. T.; Herzfeld, J.; Griffin, R. G., Cross polarization in the tilted frame: assignment and spectral simplification in heteronuclear spin systems. *Molecular Physics* **1998,** *95* (6), 1197-1207.
34. Fung, B. M.; Khitrin, A. K.; Ermolaev, K. An Improved Broadband Decoupling Sequence for Liquid Crystals and Solids. *Journal of Magnetic Resonance* **2000,** *142*, 97-101.
35. Weingarth, M.; Demco, D. E.; Bodenhausen, G.; Tekely, P., Improved magnetization transfer in solid-state NMR with fast magic angle spinning. *Chemical Physics Letters* **2009,** *469* (4-6), 342-348.
36. Baldus, M., Correlation Experiments for Assignment and Structure Elucidation of Immobilized Polypeptides Under Magic Angle Spinning. *Prog. Nucl. Magn. Reson. Spectr* **2002,** *1-47* (1-2).
37. Baldus, M.; Meier, B. H., Total Correlation Spectroscopy in the Solid State. The Use of Scalar Couplings to Determine the Through-Bond Connectivity. *Journal of Magnetic Resonance, Series A* **1996,** *121* (1), 65-69.
38. Gareth, A. M; Freeman, R., Enhancement of nuclear magnetic resonance signals by polarization transfer. *J. Am. Chem. Soc* **1979,** *101* (3), 760–762.
39. Goddard, T.; Kneller, D., SPARKY. *University of California, San Francisco*.
40. Arnold, K.; Bordoli, L.; Kopp, J.; Schwede, T., The SWISS-MODEL workspace: a web-based environment for protein structure homology modelling. *Bioinformatics* **2006,** *22* (2), 195-201.

41. Natali, A.; Croce, R., Characterization of the major light-harvesting complexes (LHCBM) of the green alga Chlamydomonas reinhardtii. *PLoS One* **2015,** *10* (2), e0119211.
42. Han, B.; Wishart, D. S.; Liu, Y.; Ginzinger, S. W., SHIFTX2: significantly improved protein chemical shift prediction. *J Biomol NMR* **2011,** *50*, 43-57.
43. Gradmann, S.; Ader, C.; Dittmann, M.; Engelhard, M.; Heinrich, I.; Cukkemane, A.; Baldus, M.; Nand, D.; Dijk, M. v.; Bonvin, A. M. J. J., Rapid prediction of multi-dimensional NMR data sets. *J Biomol NMR* **2012,** *54*, 377-387.
44. Drop, B.; Webber-Birungi, M.; Yadav, S. K. N.; Filipowicz-Szymanska, A.; Fusetti, F.; Boekema, E. J.; Croce, R., Light-harvesting complex II (LHCII) and its supramolecular organization in Chlamydomonas reinhardtii. *Biochimica et Biophysica Acta (BBA) - Bioenergetics* **2014,** *1837* (1), 63-72.
45. Ferrante, P.; Ferrante, P.; Ballottari, M.; Bonente, G.; Giuliano, G.; Bassi, R., LHCBM1 and LHCBM2/7 Polypeptides, Components of Major LHCII Complex, Have Distinct Functional Roles in Photosynthetic Antenna System of Chlamydomonas reinhardtii. *Journal of biological chemistry* **2012,** *287* (20), 16276-16288.
46. Azadi Chegeni, F.; Perin, G.; Sai Sankar Gupta, K. B.; Simionato, D.; Morosinotto, T.; Pandit, A., Protein and lipid dynamics in photosynthetic thylakoid membranes investigated by in-situ solid-state NMR. *Biochim Biophys Acta* **2016,** *1857* (12), 1849-1859.
47. Ward, M. E.; Ritz, E.; Ahmed, M. A.; Bamm, V. V.; Harauz, G.; Brown, L. S.; Ladizhansky, V., Proton detection for signal enhancement in solid-state NMR experiments on mobile species in membrane proteins. *J Biomol NMR* **2015,** *63* (4), 375-88.
48. Wang, Y.; Jardetzky, O., Investigation of the neighboring residue effects on protein chemical shifts. *Journal of the American Chemical Society* **2002,** *124* (47), 14075-84.
49. de Souza, L. M.; Iacomini, M.; Gorin, P. A.; Sari, R. S.; Haddad, M. A.; Sassaki, G. L., Glyco- and sphingophosphonolipids from the medusa Phyllorhiza punctata: NMR and ESI-MS/MS fingerprints. *Chem Phys Lipids* **2007,** *145* (2), 85-96.
50. Seiwert, D.; Witt, H.; Janshoff, A.; Paulsen, H., The non-bilayer lipid MGDG stabilizes the major light-harvesting complex (LHCII) against unfolding. *Scientific Reports* **2017,** *7* (1), 5158.
51. Azadi-Chegeni, F.; Schiphorst, C.; Pandit, A., In vivo NMR as a tool for probing molecular structure and dynamics in intact Chlamydomonas reinhardtii cells. *Photosynthesis Research* **2018,** *135* (1), 227-237.
52. Sculley, M. J.; Duniec, J. T.; Thorne, S. W.; Chow, W. S.; Boardman, N. K., The stacking of chloroplast thylakoids: Quantitative analysis of the balance of forces between thylakoid membranes of chloroplasts, and the role of divalent cations. *Archives of Biochemistry and Biophysics* **1980,** *201* (1), 339-346.
53. Su, X.; Ma, J.; Wei, X.; Cao, P.; Zhu, D.; Chang, W.; Liu, Z.; Zhang, X.; Li, M., Structure and assembly mechanism of plant C2S2M2-type PSII-LHCII supercomplex. *Science (New York, N.Y.)* **2017,** *357* (6353), 815-820.